Synergetic effects of double laser pulses for the formation of mild plasma in water: Toward non-gated underwater laser-induced breakdown spectroscopy

Tetsuo Sakka, Ayaka Tamura, Takashi Nakajima, Kazuhiro Fukami, and Yukio H. Ogata

Citation: J. Chem. Phys. **136**, 174201 (2012); doi: 10.1063/1.4709391
View online: http://dx.doi.org/10.1063/1.4709391
View Table of Contents: http://jcp.aip.org/resource/1/JCPSA6/v136/i17
Published by the American Institute of Physics.

Synergetic effects of double laser pulses for the formation of mild plasma in water: Toward non-gated underwater laser-induced breakdown spectroscopy

Tetsuo Sakka,[1,2,a)] Ayaka Tamura,[1] Takashi Nakajima,[1] Kazuhiro Fukami,[1] and Yukio H. Ogata[1]
[1]*Institute of Advanced Energy, Kyoto University, Uji, Kyoto 611-0011, Japan*
[2]*Institute of Sustainability Science, Kyoto University, Uji, Kyoto 611-0011, Japan*

(Received 27 February 2012; accepted 14 April 2012; published online 3 May 2012)

We experimentally study the dynamics of the plasma induced by the double-laser-pulse irradiation of solid target in water, and find that an appropriate choice of the pulse energies and pulse interval results in the production of an unprecedentedly mild (low-density) plasma, the emission spectra of which are very narrow even without the time-gated detection. The optimum pulse interval and pulse energies are 15–30 μs and about ~1 mJ, respectively, where the latter values are much smaller than those typically employed for this kind of study. In order to clarify the mechanism for the formation of mild plasma we examine the role of the first and second laser pulses, and find that the first pulse produces the cavitation bubble without emission (and hence plasma), and the second pulse induces the mild plasma in the cavitation bubble. These findings may present a new phase of underwater laser-induced breakdown spectroscopy. © *2012 American Institute of Physics*. [http://dx.doi.org/10.1063/1.4709391]

I. INTRODUCTION

Laser-induced breakdown spectroscopy (LIBS) is a very useful technique for the spectrochemical analysis of elements.[1,2] For that purpose the production of strong and narrow spectral lines in the plasma emission is highly desired for the accurate identification of the elements. In practice, however, this is not an easy task for the samples in liquids, since the use of strong laser pulses results in the severely distorted spectral lines which cannot be appropriately identified.[3,4] Moreover, the use of weak laser pulses does not help so much, either, because the plasma plumes produced in water are confined in a very small volume, anyway, and hence the plasma emission takes place under the extremely high pressure (typically ~1 GPa),[5] where the spectral deformation occurs due to the bremsstrahlung, radiative recombination, and the Stark and collisional broadenings[6,7] as well as self-absorption.[8–10]

To overcome the difficulty for LIBS in water, double-pulse[11–13] and long-pulse[14] configurations together *with a time-gated detection* have been proposed, where the proper adjustment of the gate-timing is crucial to obtain the narrow emission lines. Note that the double-pulse and long-pulse configurations are based on the different physical mechanisms: For the former the first pulse produces a plasma and also a cavitation bubble, while the second pulse produces a plasma at the delay (typically 30−100 μs) when the bubble provides a gaseous environment for the ablation by the second pulse, and hence allows an emission of sufficiently narrow spectral lines.[12] On the other hand, for the latter a mild ablation and hence a low-density plasma is produced by the long laser pulse to obtain narrow spectral lines.[14]

In this paper we demonstrate that the very low-energy double-pulse laser ablation of a solid target in water results in surprisingly narrow emission spectral lines *without a time-gated detection* only if we optimize the pulse energies and pulse interval. The optimized pulse energies are surprisingly low (about 1 mJ or less), and accordingly the roles of the first and second pulses are found to be completely different from those of the conventional double-pulse configuration with the pulse energies of tens of mJ. We emphasize that the very narrow emission spectra in water are a strong evidence for the formation of unprecedentedly low-density plasma, which seems to suggest that we have found a new type of mechanism for the laser-induced breakdown in water. Our findings present a new phase of underwater LIBS.

II. EXPERIMENTAL

We used two flashlamp-pumped Q-switched Nd:YAG lasers (home-build) with the pulse durations of 18 ns and 16 ns for the first and second pulses, respectively, where the pulse energies were controlled by the flashlamp intensities. The delay between the two pulses was varied from 1 μs to 80 μs, and the two pulses were combined to be collinear by a glass wedge, and focused onto the metallic target (Al or Cu) placed in a water-filled quartz cell from the normal direction by a 60-mm focal length lens. Ultrapure water (Millipore, Milli-Q) was used for the experiments. The water was not degassed during the experiment, and hence, there might be some air (or oxygen) dissolved in the water. The water was replaced to a new one before the bulk breakdown due to the particles produced by the precedent pulses occurs frequently. The plasma emission was detected from the direction

a)Electronic mail: t-sakka@iae.kyoto-u.ac.jp.

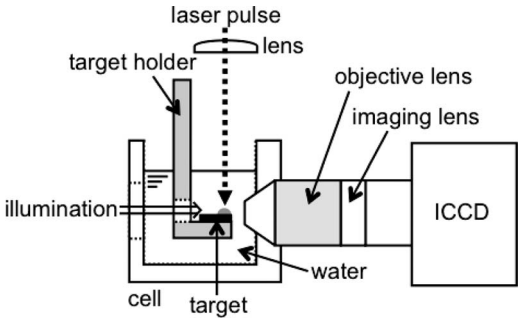

FIG. 1. Experimental setup for shadowgraphy of the cavitation bubble with simultaneous imaging of the plasma emission. A tungsten halogen lamp was used as a back illumination light source for the shadowgraphy. The time delays of the double laser pulses and the ICCD gating were controlled by a delay generator. The gate delay of the ICCD was set to be 100 ns before the second pulse with the gate width being 400 ns. This means that the most intensive part of the emission caused by the second pulse is integrated into the image.

perpendicular to the laser pulses by the spectrometer (Bunko Keiki, MT-25P) equipped with an intensified CCD (ICCD) (Roper Scientific, PI-MAX). All the timings of the two laser pulses and the gate of ICCD were controlled by the delay generator (Stanford Research Systems, DG535).

For Al atoms we observed emission lines at 394.40 nm and 396.15 nm, corresponding to the $3s^2 3p\ ^2\mathrm{P}^o_{1/2} - 3s^2 4s\ ^2\mathrm{S}_{1/2}$ and $3s^2 3p\ ^2\mathrm{P}^o_{3/2} - 3s^2 4s\ ^2\mathrm{S}_{1/2}$ transitions, respectively.[15] Since the lower level for these lines is the ground state, the emission can be immediately re-absorbed by abundant ground state atoms, and therefore the spectral lines suffer from the strong self-absorption. The linear Stark broadening parameter is 4.22×10^{-19} nm · cm^3 at 13200 K, which is typical for this class of transitions.[16]

Experimental setup for simultaneous measurement of the shadowgraphy of a cavitation bubble and the imaging of the plasma emission is shown in Fig. 1. A tungsten halogen lamp was used as a back illumination light source for the shadowgraphy. Timing of the imaging was controlled by the time-gated operation of the ICCD detector. The time delay between the two laser pulses and the delay of the ICCD gating were controlled by the delay generator, as in the case of spectral measurements.

III. RESULTS AND DISCUSSION

In Fig. 2 we present representative emission spectra obtained by the double-pulse irradiation with different pulse intervals. The left (center) column of Fig. 2 shows the spectra for different pulse intervals at the first and second pulse energies of 0.4 mJ and 1.0 mJ (0.4 mJ and 10 mJ). The gating window of the ICCD detector was set from 40 μs before the first pulse to 100 μs after the first pulse, and this is practically equivalent to the non-gated measurement. It is clear that the spectral shape is sensitive to the pulse interval, especially when the second pulse energy is low (left column of Fig. 2). Note that the deformation observed in these spectra is attributed to the high density of ablated species in the plasma.[5,9] For the pulse interval of 1 μs the spectrum is extremely broadened and shifted, and the two self-reversed lines appear at the

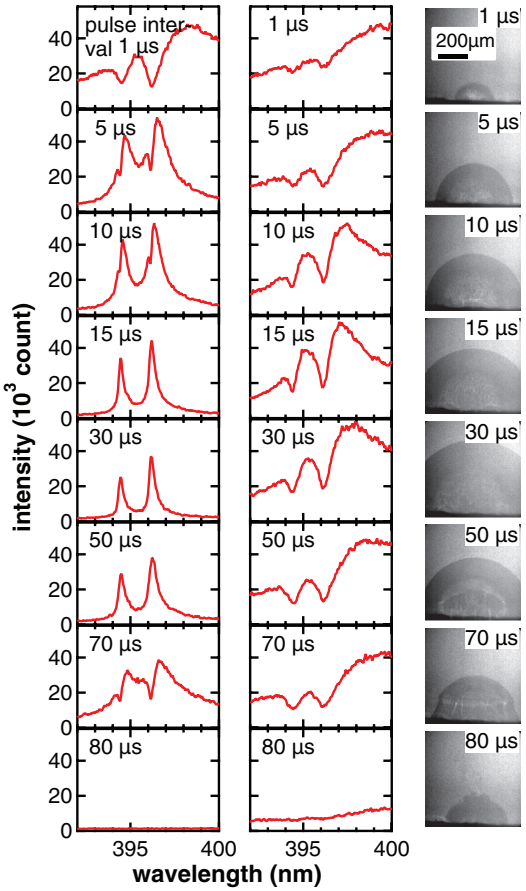

FIG. 2. (Left column) Emission spectra obtained by the irradiation of Al metal target in water by two pulses with various pulse intervals. The integration of the signal was performed in a way equivalent to the non-gated measurement. The energies of the first and second pulses were 0.4 mJ and 1.0 mJ, respectively. (Center column) Same as those in the left column but with the second pulse energy of 10 mJ. (Right column) The shadowgraph images at different delays after the first pulse. Note that the second pulse was absent when the shadowgraphs were taken.

original wavelengths of the transition, which is very similar to the one obtained by the single pulse irradiation or the double-pulse irradiation at higher pulse energies without optimization of the gate-timing for detection. For the pulse interval of ~15 μs the spectral deformation appears minimal. The spectrum obtained by the pulse interval of 80 μs shows no signal. This means that the first pulse with the pulse energy of 0.4 mJ does not give any emissive plasma by itself. The first pulse only assists the second pulse to produce plasma, and the assistance is effective only when the pulse interval is appropriate. If we use a higher pulse energy for the second pulse, say, 10 mJ, the spectral deformation turned out to be much more serious (center column of Fig. 2), and we could not find any pulse interval to minimize the spectral deformation. For the intuitive understanding for the role of the first pulse we perform the shadowgraphy to image the cavitation bubble formed after the first pulse. The results are shown in the right column of Fig. 2. We can see that the size of the bubble expands with time and after it reaches the maximum size at the delay of 15–50 μs, it shrinks. It should be noted that we have not observed light emission at the collapse of the bubble, probably because the laser power was too low for the bubble to have

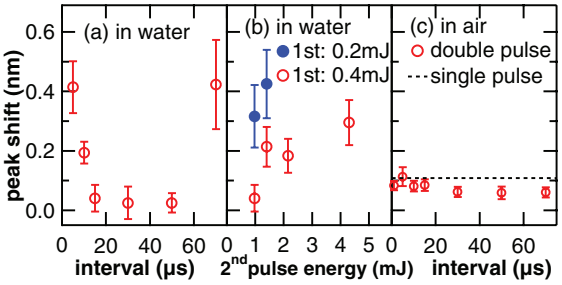

FIG. 3. Peak shift of the 396 nm line for the Al target in water as a function of (a) pulse interval and (b) energy of the second pulse. (c) Similar to (a) but in air. For (a) and (c) the first and second pulse energies were 0.4 mJ and 1.0 mJ, respectively. In (b) the results with the first pulse energies of 0.4 mJ and 0.2 mJ were shown by open and closed circles, respectively. In (c) the shifts obtained by a single 0.4-mJ-pulse irradiation is indicated by a broken line.

sufficient energy for the light emission when it collapses. This is favorable for non-gated measurement. Later on in this paper we will make further discussion for the role of the cavitation bubble.

To be more quantitative we plot the peak shift for the 396 nm line as a function of pulse interval and second pulse energy. The results are shown in Figs. 3(a) and 3(b), respectively. Since the shift is primarily caused by the collisional and Stark effects,[6] the shift of the 394 nm line shows a behavior very similar to that of the 396 nm line, and hence we do not show it. As we see in Fig. 3(a), the emission peak is always redshifted. It is obvious that the pulse intervals from 15 to 50 μs result in the considerably small shifts. Note that these pulse intervals correspond to the delay when the size of the cavitation bubble reaches the maximum as we mentioned before. For the pulse intervals shorter or longer than this "optimum range" the spectral deformation is significant. Thus, the spectral deformation is well correlated with the shift: When the shift is small the spectral deformation is also small, and vice versa. Interestingly, the shift of the peak depends not only on the pulse interval but also on the second pulse energy, as shown in Fig. 3(b), where the first pulse energy was fixed to 0.2 mJ or 0.4 mJ, while the second pulse energy was varied from 1.0 mJ to 4.5 mJ. The pulse interval was fixed to be 15 μs. Although the first pulse alone did not produce any plasma emission if the pulse energy is 0.2 mJ or 0.4 mJ, an introduction of the second pulse at the pulse interval of 15 μs produced the plasma emission. Moreover, the shift becomes larger as the second pulse energy increases. Note, however, that the energy of the first pulse should not be too low. If it is too low, say, 0.2 mJ, we found that the shift of the peak is significantly large, i.e., the emission spectra are considerably deformed irrespective of the second pulse energy, suggesting that the effect of the first pulse is not enough. Clearly, there is an optimized set of values for the first and second pulse energies. For comparison Fig. 3(c) shows the shift of the Al 396 nm line in air as a function of pulse interval. All the experimental conditions were the same as Fig. 3(a), except for the presence of air instead of water. Narrow spectral lines were always observed irrespective of the pulse interval, and also for the single pulse irradiation. This implies that the dynamics in air is essentially different from that in water, where the double pulse is essential to observe narrow spectral lines.

From the results shown in Figs. 2 and 3, we consider that the narrow (less-deformed) emission spectra in water by the low-energy double pulses is due to a *synergetic effect of the first and second pulses*. Namely, it seems that the role of the first pulse is to form a cavitation bubble[17,18] without emission (and hence plasma), the size of which will reach the maximum at 15–50 μs after the first pulse, to heat the surface, and/or to weakly evaporate the surface species.[19] Among them the formation of the cavitation bubble seems to be most important, since it provides a low-pressure (gaseous) region which may be used to contain the relatively low-density plasma. The formation of the bubble is also considered to be important for the conventional high power double pulse LIBS,[12,13,20] i.e., the ablation by the second pulse in the gaseous environment provided by the bubble is essential for the observation of well-defined atomic lines. Recall that there is a clear coincidence in terms of the delay time to observe the minimum shift of the peak (Fig. 3(a)) and the maximum size for the cavitation bubble (right column of Fig. 2). Along this interpretation for the role of the first pulse, the role of the second pulse is to induce a plasma. Note, however, that the second pulse energy we employed in this work is not sufficient in the absence of the first pulse. This implies that the ablation threshold in terms of the incident pulse energy is significantly lowered by the first pulse so that the second pulse, whose energy alone is not sufficient to induce plasma, can induce plasma. We point out that the effect of the first pulse does not last longer than 50 μs, as Fig. 3(a) suggests. The fact that the observed emission spectra are very narrow implies that the plasma density induced by the second pulse is surprisingly low. Up to this point, however, we still do not know whether it is the solid target or something in the cavitation bubble that the second pulse interacts to form the plasma. A simultaneous measurement of the emission spectra and the cavitation bubble with temporal as well as spatial resolutions is highly desired to draw more definitive conclusions.

In order to draw more definitive conclusions we have performed the experiment to simultaneously image the visible emission by the second pulse and the cavitation bubble produced by the first pulse at the arrival time of the second pulse. The results are shown in Fig. 4. Note that the bubble image is usually overwhelmed by the very bright plasma emission by the second pulse, and hence very difficult to obtain. In order to overcome this difficulty the bubble was illuminated by the intense light from behind to image the shadow of the bubble. The signal was integrated with the ICCD camera from 100 ns before the second pulse to 400 ns after the second pulse. The pulse interval was chosen to be 15 μs to compare with the fourth spectrum in the left column of Fig. 2. Figure 4 clearly shows that the major part of the emission is sitting well inside the bubble, and the spatial contact with the bubble boundary seems to be minimal. Similar images were obtained for the pulse interval of 30–50 μs in which we can always obtain the narrow spectral lines. When the pulse interval is shorter than 15 μs or longer than 50 μs the size of the bubble is smaller than that of the plasma plume (not shown here), meaning that the emission takes place also in the high-density region.

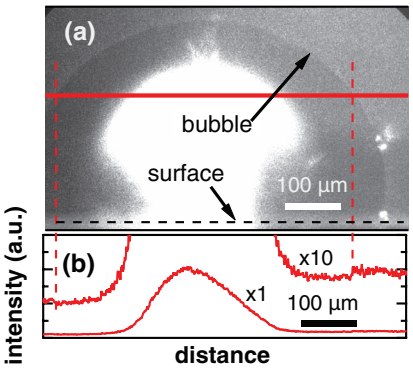

FIG. 4. (a) Simultaneous imaging of the emission region and cavitation bubble into a single photograph. The Al target in water was irradiated by the two pulses with the energies of 0.8 mJ (first pulse) and 1.0 mJ (second pulse) with a pulse interval of 15 μs. The photograph was obtained by the ICCD camera with the gate window from 100 ns before the second pulse to 400 ns after the second pulse. The intensity profile along the solid red line shown in (a) is given in (b) by averaging over the 10 adjacent pixels. To clearly see the boundary of the bubble, a magnified profile is also shown in (b).

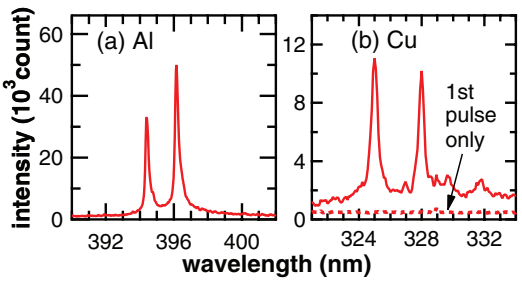

FIG. 5. Emission spectra obtained by using a multi-pulse microchip laser as an excitation source. (a) Al and (b) Cu as targets in water. The solid lines in (a) and (b) were obtained with the gate which started 40 μs before the first pulse lasts for 300 μs, and hence the entire emission was integrated. The dotted line in (b) was obtained with the gate which started 500 ns after the first pulse and lasts for 10 μs, and hence the emission induced by the first pulse only was integrated.

This could be the reason for the serious deformation of the spectra.

We also tried the double-pulse experiment with an intentional spatial misalignment of the irradiation spots of the first and second pulses. When the misalignment was 60 μm which is comparable to the laser spot size, we observed the significant decrease in the spectral intensity, and when it was 90 μs we could not observe the spectrum anymore. These findings indicate that the role of the second pulse is not to interact with the bubble (>200 μm, see Fig. 2) which is much larger than the laser spot size, but to interact with the exact position of the target where the first pulse has irradiated. The fact that the first and second pulses must have the exact spatial overlap suggests that the bubble formation by other means such as ultrasonic irradiation or boiling by bulk heating of the target, etc., could not be a replacement of the first pulse.

Based on the roles of the first and second pulses we have clarified above it is now clear why there exist optimum conditions for the pulse energies and pulse intervals to obtain the well-defined narrow spectra in water with non-gated measurements: The energy of the first pulse should be sufficiently high to produce a large bubble so that it can contain the plasma plume, which is to be induced by the second pulse, without contacting to bulk water, but it should not be too high to avoid the immediate production of the plasma. The second pulse should be turned on at the moment when the size of the bubble is maximum to provide the large gaseous space for the plasma plume which is to be produced by the second pulse, and its energy should not be too high, otherwise the space provided by the bubble is not sufficient for the plasma plume, resulting in the formation of high-density plasma and hence the spectra are severely deformed.

The above results for the double-pulse configuration suggest that the double-pulse light source may be conveniently replaced by a low-energy multi-pulse laser. The great advantage of such a replacement is that the pointing, divergence, and diameter of sequential pulses from a single laser oscillator are identical. Overlap of the laser spots on the target is automatically guaranteed. We have performed the similar experiments using a multi-pulse microchip laser (proto-type) of Hamamatsu Photonics Inc. as a light source. The laser provides 10–12 pulses in one sequence with the pulse interval of ~15 μs, and each pulse has a 3 ns duration with ~0.5 mJ energy. The laser was operated at 1 Hz, and the total energy of one pulse sequence was 6 mJ. The results for the Al and Cu targets placed in water are shown in Fig. 5. For Fig. 5(a) and the solid line of Fig. 5(b) we chose the gate which starts 40 μs before the first pulse and lasts for 300 μs. This means that the entire emission induced by one pulse sequence was integrated, which is practically equivalent to the non-gated measurement. As expected the spectral lines are very sharp with negligible shifts of the peaks. To further confirm the consistency with our results by the double-pulse configuration, we also took the spectrum for the Cu target by applying an appropriate gate to collect the emission solely from the first pulse. The results are shown by the dashed line in Fig. 5(b). It clearly shows that the emission is induced not by the first pulse but by the following pulses.

IV. CONCLUSIONS

We have found that the dynamics of plasma formation by irradiating a solid target in water with low-energy double laser pulses is quite different from the conventional high-energy double pulse irradiation. Namely, if the pulse energies and pulse interval are appropriately chosen, the first pulse produces a cavitation bubble *without plasma*, and the second pulse induces plasma by interacting with the exact position of the solid target irradiated by the first pulse to produce plasma plume *within the bubble*. As a result the density of the produced plasma is very low, which enables us to obtain well-defined narrow spectral lines by non-gated measurement. This is in contrast to the existing double-pulse experiments which typically utilize the pulse energies of several tens of mJ or more, and moreover the time-gated detection is always needed to obtain well-defined spectra. Finally, the fact that our experimental configuration requires neither bulky time-resolved detection system nor high-power laser system offers a great advantage for the practical application of the present technique to *on-site* underwater laser-induced breakdown spectroscopy.

ACKNOWLEDGMENTS

This work was financially supported partly by KAKENHI (23560023) and partly by Mobile Site Research Program of ISS, Kyoto University.

[1]D. A. Cremers and L. J. Radziemski, *Handbook of Laser-Induced Breakdown Spectroscopy* (Wiley, Chichester, 2006).
[2]A. W. Miziolek, V. Palleschi, and I. Schechter, *Laser-Induced Breakdown Spectroscopy, Fundamentals and Applications* (Cambridge University Press, Cambridge, England, 2006).
[3]T. Sakka, K. Takatani, Y. H. Ogata, and M. Mabuchi, J. Phys. D **35**, 65 (2002).
[4]H. Yui and T. Sawada, Phys. Rev. Lett. **85**, 3512 (2000).
[5]K. Saito, K. Takatani, T. Sakka, and Y. H. Ogata, Appl. Surf. Sci. **197–198**, 56 (2002).
[6]H. R. Griem, *Principles of Plasma Spectroscopy* (Cambridge University Press, Cambridge, England, 1997).
[7]T. Sakka, S. Iwanaga, Y. H. Ogata, A. Matsunawa, and T. Takemoto, J. Chem. Phys. **112**, 8645 (2000).
[8]R. D. Cowan and G. H. Dieke, Rev. Mod. Phys. **20**, 418 (1948).
[9]T. Sakka, T. Nakajima, and Y. H. Ogata, J. Appl. Phys. **92**, 2296 (2002).
[10]O. Renner, F. M. Kerr, E. Wolfrum, J. Hawreliak, D. Chambers, S. J. Rose, J. S. Wark, H. A. Scott, and P. Patel, Phys. Rev. Lett. **96**, 185002 (2006).
[11]R. Nyga and W. Neu, Opt. Lett. **18**, 747 (1993).
[12]A. E. Pichahchy, D. A. Cremers, and M. J. Ferris, Spectrochim. Acta, Part B **52**, 25 (1997).
[13]A. De Giacomo, M. DellfAglio, O. De Pascale, and M. Capitelli, Spectrochim. Acta, Part A **62**, 721 (2007).
[14]T. Sakka, H. Oguchi, S. Masai, K. Hirata, Y. H. Ogata, M. Saeki, and H. Ohba, Appl. Phys. Lett. **88**, 061120 (2006).
[15]P. L. Smith, C. Heise, J. R. Esmond, and R. L. Kurucz, Atomic Spectral Line Database, *1995 Atomic Line Data (R. L. Kurucz and B. Bell) Kurucz CD-ROM No. 23, Smithsonian Astrophysical Observatory, Cambridge, MA*; see http://www.cfa.harvard.edu/amp/ampdata/kurucz23/sekur.html.
[16]N. Konjevic, M. S. Dimitrijevic, and W. L. Wiese, J. Phys. Chem. Ref. Data **13**, 619 (1984).
[17]H. C. Chu, S. Vo, and G. A. Williams, Phys. Rev. Lett. **102**, 204301 (2009).
[18]W. Soliman, T. Nakano, N. Takada, and K. Sasaki, Jpn. J. Appl. Phys. **49**, 116202 (2010).
[19]M. von Allman and A. Blatter, *Laser-Beam Interactions with Materials*, *Physical Principles and Applications*, 2nd ed. (Springer-Verlag, Berlin, 1994).
[20]A. De Giacomo, M. Dell'Aglio, F. Colao, and R. Fantoni, Spectrochim. Acta, Part B **59**, 1431 (2004).